Modeling long-range memory with stationary Markovian processes

Salvatore Micciché
Dipartimento di Fisica e Tecnologie Relative, Università degli Studi di Palermo, Viale delle Scienze, Ed. 18, I-90128 Palermo, Italy
(Received 5 June 2008; revised manuscript received 6 January 2009; published 23 March 2009)

In this paper we give explicit examples of long-range correlated stationary Markovian processes $y(t)$ where the stationary probability density function (pdf) shows tails which are Gaussian or exponential. These processes are obtained by simply performing appropriate coordinate transformations of a specific power–law correlated additive process $x(t)$, already known in the literature, whose pdf shows power-law tails. We give analytical and numerical evidences that although the new processes are Markovian and have Gaussian or exponential tails, their autocorrelation function shows a power-law decay with logarithmic corrections. For a generic continuous and monotonously increasing coordinate transformation, we also analytically investigate what is the relationship between the asymptotic decay of the autocorrelation function and the tails of the stationary pdf. Extreme events seem to be associated to long-range correlated processes with power-law decaying autocorrelation function. However, the occurrence of extreme events is not necessary in order to have more general long-range correlated processes in which the autocorrelation shows a slow decay characterized by a power-law times a correction function such as the logarithm. Our results help in clarifying that even in the context of stationary Markovian processes long-range dependencies are not necessarily associated to the occurrence of extreme events. Moreover, our results can be relevant in the modeling of complex systems with long memory. In fact, we provide simple stationary processes associated to Langevin equations with white noise thus confirming that long-memory effects can be modeled in the context of continuous time stationary Markovian processes.

DOI: 10.1103/PhysRevE.79.031116 PACS number(s): 02.50.Ey, 05.10.Gg, 05.40.−a, 02.50.Ga

I. INTRODUCTION

Stochastic processes have been used to model a great variety of systems in disciplines as disparate as physics [1–6], genomics [7,8], finance [9,10], climatology [11], and social sciences [12]. One possible classification of stochastic processes takes into account the properties of their conditional probability densities. In this respect, Markov processes play a central role in the modeling of natural phenomena. In the framework of discrete time stochastic processes, a process $x(t)$ is said to be a Markov process if the conditional probability density $P(x_{n+1},t_{n+1}|x_n,t_n;\ldots;x_1,t_1)$ depends only on the last value x_n at t_n and not on the previous values x_{n-1} at t_{n-1}, x_{n-2} at t_{n-2}, etc. More generally, the transition probability of any Markov process fulfills the Chapman-Kolmogorov equation [2]. It is worth noticing that a Markov process is fully determined by the knowledge of the probability density function (pdf) $W(x,t)$ of the process and the transition probability $P(x_{n+1},t_{n+1}|x_n,t_n)$. When the Markovian process is continuous both in space and time, the time evolution of the pdf is described by a Fokker-Planck (FP) equation. Such level of simplicity is rather unique among stochastic processes. In fact, a non-Markovian process is characterized by an infinite hierarchy of transition probabilities. In this case, the time evolution of the pdf is described by a master equation rather than a simpler FP equation.

Another classification of stochastic processes considers the nature of correlation of the random variable. Under this classification, random variables are divided in short-range and long-range correlated variables. Short-range correlated variables are characterized by a finite mean of time scales of the process whereas a similar mean time scale does not exist for long-range correlated variables [13]. An equivalent definition can be given by considering the finiteness or infiniteness of the integral of the autocorrelation function of the random process [14–16]. In the presence of long-range correlation, the time integral $s(t)$ of the process $x(t)$ can show anomalous diffusion [17,18]. In the case we will consider in this paper, $s(t)$ is a superdiffusive stochastic process showing $\langle|\Delta s(t)|^2\rangle \sim D_\gamma t^\gamma$ where $\gamma > 1$ and D_γ is a constant. Superdiffusive stochastic processes have been observed in several physical systems. A classical example is Richardson's observation that the relative separation ℓ of two particles moving in a turbulent fluid at time t follows the relation $\langle \ell^2(t)\rangle \propto t^3$ [19]. Other examples include anomalous kinetic in chaotic dynamics due to flights and trapping [20], dynamics of aggregate of amphiphilic molecules [21], dynamics of a tracer in a two-dimensional rotating flow [22], noncoding regions of complete genomes [23], and volatility in financial markets [24].

In the context of stochastic processes which admit a generalized Langevin equation, several non-Markovian [25–29] or nonstationary [30] models of long-range correlated and anomalous diffusing processes have been developed. However, these models mostly rely on generalizations of the Langevin equation or FP equation as to include convolutions with memory kernels or the use of fractional derivatives. In this paper we will consider the issues of long-range correlation and anomalous diffusion in the context of stochastic stationary Markovian processes that can be described by a nonlinear Langevin equation, with a white-noise term, and a FP equation.

Several stationary Markovian processes are short-range correlated. In fact, the paradigmatic Markovian process is the Ornstein-Uhlembeck (OU) one [31], whose autocorrelation function is the exponential function $\rho(\tau)=e^{-\tau/T}$, where T is the time scale of the process. Although in the OU process

there is one single time scale, a general Markovian stationary process can be multiscale, i.e., it may admit either a discrete or a continuum set of time scales. In the last case, when the largest time scale is removed to infinity the process can even be long-range correlated. The paradigmatic Markovian process with power-law autocorrelation function is given by the family of processes considered in Ref. [32]. These are stationary Markovian power-law correlated processes that were introduced in the context of diffusion in optical lattices and semiclassically describe the motion of atoms in a one-dimensional optical lattice formed by two counterpropagating laser beams perpendicularly polarized. For a certain choice of the relevant parameters the processes become long-range correlated.

The existence of a power-law-decaying autocorrelation function in the processes of Ref. [32] is intimately related to the existence of power-law tails in the stationary pdf. This is easily understood by considering that the processes of Ref. [32] describe particles moving in a confining Smoluchowski potential which asymptotically grows like $\log(x)$. If one compares such slow growth with the one associated to the OU process, whose Smoluchowski potential grows like x^2, it is easy to recognize that in the case of Ref. [32] (i) a particle can reach positions far away from the center of the potential because it is subject to a relatively weaker force and (ii) if a particle reaches a position X, then it is not suddenly recalled toward the center of the potential and therefore it can explore for relatively long times the regions around X. Loosely speaking, the time series of the processes of Ref. [32] can show persistencies and clustering of extreme events. The theory of extreme events is a consolidated area of research. The literature in this field can be traced back to the pioneering work of Gumbel and Gnedenko [33,34] and currently finds applications in fields such as finance and natural and social sciences [35,36].

In this context, the processes mentioned above perfectly fit the features of the model proposed in Ref. [37], where long-range dependencies are shown to explain the clustering of extreme events in climate records. However, one could have in principle slowly decaying autocorrelation functions without necessarily observing the occurrence of extreme events. One such example is given by the Fractional Brownian motion (FBm) [13], which is a stochastic process where the autocorrelation function decays like a power law and the stationary pdf is Gaussian. We are here interested in understanding whether also in the context of stationary Markovian processes it is possible to have long-range correlation without necessarily observing the occurrence of extreme events. In this paper we give explicit examples of long-range correlated stationary Markovian processes where the stationary pdf shows tails which are Gaussian or exponential. We will introduce such processes starting from appropriate coordinate transformations of an additive processes introduced in Ref. [32].

The paper is organized as follow. In Sec. II we review the eigenfunction methodology used to analyze the correlation properties of a given stochastic process and introduce a specific power-law correlated process with power-law tails in the stationary pdf. In Secs. III and IV we present examples of long-range correlated stochastic processes with Gaussian and exponential tails in the stationary pdf respectively. In Sec. V we present an analytical argument that shows how the asymptotic decay of the autocorrelation function is linked with the tails of the stationary pdf. In Sec. VI we finally draw our conclusions.

II. POWER-LAW TAILS IN THE PDF

In this section we briefly review the family of stochastic processes introduced in Ref. [32] and whose ergodicity properties have been investigated in Ref. [38]. A similar class of such processes has been considered in Ref. [39].

Let us consider a continuous stationary Markovian stochastic process $x(t)$ whose pdf $W(x,t)$ is described by the FP equation with constant diffusion coefficient $\partial_t W=-\partial_x[D^{(1)}(x)W]+D\partial_x^2 W$. For the sake of simplicity, in this study we set $D=1$. In general, the eigenvalue spectrum of the FP equation describing a stationary process consists of a discrete part $\lambda_0=0,\lambda_1,\ldots,\lambda_p$ and a continuous part $]\lambda_c,+\infty[$ $(\lambda_c\geq\lambda_p)$ associated with eigenfunctions φ_λ. The stationary pdf is $W(x)=\varphi_0$. The FP equation with constant diffusion coefficient can be transformed into a Schrödinger Eq. (3) with a quantum potential $V_S(x)=[D^{(1)}(x)]^2/4+\partial_x D^{(1)}(x)/2$. The eigenvalue spectrum of the Schrödinger equation is equal to the eigenvalue spectrum of the FP equation. The relation between the eigenfunctions of the FP equation and the eigenfunctions ψ_λ of the Schrödinger equation is $\varphi_\lambda=\psi_\lambda\psi_0$. For a stationary process the two-point probability density function $W_2(x,t;x',t+\tau)$ can be expressed in terms of the eigenfunctions of the Schrödinger equation. Specifically, one can write

$$W_2(x,t;x',t+\tau)=\psi_0(x)\psi_0(x')\left(\sum_{\lambda=\lambda_1}^{\lambda_p}\psi_\lambda(x)\psi_\lambda(x')e^{-\lambda\tau}+\int_{\lambda_c}^{+\infty}d\lambda\,\psi_\lambda(x)\psi_\lambda(x')e^{-\lambda\tau}\right). \quad (1)$$

Equation (1) extends the analogous expression valid for a FP equation with only discrete spectrum [3] to the case in which there also exists a continuous part of the spectrum. By direct inspection, it can be shown that W_2 fulfills the Chapman-Kolmogorov equation. In order to evaluate the autocorrelation function $\rho(\tau)=[\langle x(t+\tau)x(t)\rangle-\langle x(t)\rangle^2]/[\langle x^2(t)\rangle-\langle x(t)\rangle^2]$ of the stochastic variable $x(t)$, we make use of the expression

$$\langle x(t+\tau)x(t)\rangle=\sum_{\lambda=\lambda_1}^{\lambda_p}C_\lambda^2 e^{-\lambda\tau}+\int_{\lambda_c}^{+\infty}C_\lambda^2 e^{-\lambda\tau}d\lambda, \quad (2)$$

where $C_\lambda\equiv\int dx x\varphi_\lambda(x)$. Equation (2) follows from Eq. (1) and from the definition of the autocovariance function

$$\langle x(t+\tau)x(t)\rangle=\int\int_{-\infty}^{+\infty}dx'dx x'xW_2(x,t;x',t+\tau). \quad (3)$$

Equation (2) holds true under the assumption that the integrations in $\int dx'$, $\int dx$, and $\int d\lambda$ can be interchanged.

The asymptotic temporal dependence of the autocorrelation function can have a different behavior conditioned by

the properties of the eigenvalue spectrum [40–43]. Specifically, following [44] one can distinguish three different cases, depending on the existence of a continuum spectrum of eigenvalues and whether or not such spectrum is attached to the ground state.

In fact, the class of processes introduced in Ref. [32] belongs to the one admitting a continuum part of the spectrum attached to the ground state. In this paper we will consider the specific stationary Markovian processes associated with a quantum potential V_S given by

$$V_S(x) = \begin{cases} -V_0 & \text{if } |x| \le L \\ V_1/x^2 & \text{if } |x| > L, \end{cases} \tag{4}$$

where L, V_0, and V_1 are positive constants. The reason for considering such specific potential, among all those fulfilling the requirements of Ref. [32], is that it is exactly solvable and therefore it will allow us to perform most calculations analytically.

The parameters L, V_0, and V_1 can be chosen in such a way that the spectrum contains one single discrete eigenvalue $\lambda_0=0$ and a continuous part for $\lambda>0$. As a result, the parameters L, V_0, and V_1 are not independent. In fact, the continuity of $\partial_x\psi_0$ in $x=L$ provides a relation between them. The Langevin equation of the process is

$$\dot{x} = h(x) + dz,$$

$$h(x) = \begin{cases} -2\sqrt{V_0}\tan(\sqrt{V_0}x) & \text{if } |x| \le L \\ (1-\sqrt{1+4V_1})/x & \text{if } |x| > L, \end{cases}$$

$$V_1 = L\tan(\sqrt{V_0}L)[1 + L\tan(\sqrt{V_0}L)]. \tag{5}$$

The associated FP equation describes the dynamics of an overdamped particle moving in a Smoluchowski potential $U(x)=-\int dx h(x)$ that increases logarithmically in x. For $|x|\le L$, the eigenfunction of the ground state is $\psi_0=B_0\cos(\sqrt{V_0}x)$ whereas for $|x|>L$ it decays according to $\psi_0=A_0x^{(1-\sqrt{1+4V_1})/2}$. The constants A_0 and B_0 are set by imposing that ψ_0 is normalized and continuous in $x=L$. It is worth noting that for $|x|>L$ the stationary pdf $W(x)$ of the stochastic process is a power-law function decaying as $|x|^{-\alpha}$ with $\alpha=\sqrt{1+4V_1}-1$. The normalizability of the eigenfunction of the ground state is ensured if $\alpha>1$. In the present study we consider stochastic processes with finite variance which implies $\alpha>3$. Due to parity arguments, only the odd eigenfunctions $\psi_\lambda^{(\mathrm{odd})}$ of the continuous spectrum give a nonvanishing contribution to C_λ. For $|x|>L$ the eigenfunction $\psi_\lambda^{(\mathrm{odd})}$ is a linear combination of Bessel functions $\psi_\lambda^{(\mathrm{odd})}=A_\lambda\sqrt{x}J_\nu(\sqrt{\lambda}x)+B_\lambda\sqrt{x}Y_\nu(\sqrt{\lambda}x)$, where $\nu=(\alpha+1)/2$. For $|x|\le L$ we find $\psi_\lambda^{(\mathrm{odd})}=D_\lambda\sin(\sqrt{V_0+\lambda}x)$. The coefficients A_λ, B_λ, and D_λ are fixed by imposing that $\psi_\lambda^{(\mathrm{odd})}$ and its first derivative are continuous in $x=L$ and that $\psi_\lambda^{(\mathrm{odd})}$ are orthonormalized with a δ function of the energy. Similar conditions apply to the even solutions.

By using these eigenfunctions we obtain an exact expression for C_λ. The further integration required in Eq. (2) to obtain $\langle x(t+\tau)x(t)\rangle$ cannot be performed analytically. By using Watson's lemma [45] and by considering that the first term of the Taylor expansion of C_λ^2 is proportional to $\lambda^{(\alpha-5)/2}$ for small values of λ, for large values of τ one gets $\langle x(t+\tau)x(t)\rangle\propto\tau^{-\beta}$, where $\beta=(\alpha-3)/2$. That indicates that this stochastic process is stationary, Markovian, and asymptotically power-law autocorrelated. When $3<\alpha<5$ the process is long-range correlated.

III. GAUSSIAN TAILS IN THE PDF

In this section we explicitly present a stationary Markovian process with a slowly decaying autocorrelation function and a stationary pdf with Gaussian tails. In fact, let us consider the coordinate transformation

$$f_g(x) = \begin{cases} \sqrt{2s}\,\mathrm{Erf}^{-1}[(1-a(x))\mathrm{Erf}(Lr/\sqrt{2s}) + a(x)(1+\nu)] & x > L \\ -\sqrt{2s}\,\mathrm{Erf}^{-1}[(1-a(-x))\mathrm{Erf}(Lr/\sqrt{2s}) + a(-x)(1+\nu)] & x < -L \\ rx & |x| \le L, \end{cases}$$

$$\nu = \frac{Lr\sqrt{V_0}\,\sec(L\sqrt{V_0})^2 + r\tan(L\sqrt{V_0})}{\sqrt{2\pi s V_0}e^{L^2r^2/2s}},$$

$$a(x) = \frac{2A_0^2(Lx^\alpha - xL^\alpha)}{(\alpha-1)L^\alpha x^\alpha}$$

where r is a real positive constant. It is straightforward to prove that f_g is continuous and monotonic. By using the Ito lemma, one can show that starting from the process of Eq. (5), in the coordinate space $y=f_g(x)$ one gets a multiplicative stochastic process whose stationary pdf is

$$W_g(y) = \begin{cases} N_{\mathrm{I}}e^{-1/2sy^2} & |y| > Lr \\ N_{\mathrm{II}}\cos(\sqrt{V_0}y/r) & |y| \le Lr, \end{cases} \tag{6}$$

where N_{I} and N_{II} are normalization constants that can be analytically computed by imposing that $W_g(y)$ is continuous

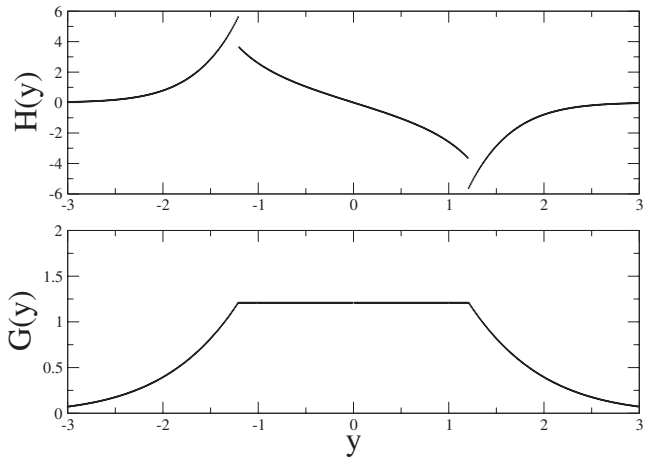

FIG. 1. The figure shows the drift coefficient $H(y)$ (top panel) and diffusion coefficient $G(y)$ (bottom panel) of the process defined by the coordinate transformation of Eq. (6) for the case when $L=1.0$, $V_0=0.987$ (i.e., $\alpha=3.05$), and $s=1.0$ (i.e., $r=1.2096$).

in $y=\pm Lr$ and it is normalized to unity. The real constant r is fixed by imposing that the diffusion coefficient $G(y)$ of the multiplicative stochastic process in the y coordinate space is continuous in $y=\pm Lr$. In Fig. 1 we show the drift coefficient $H(y)$ (top panel) and diffusion coefficient $G(y)$ (bottom panel) for the case when $L=1.0$, $V_0=0.987$ (i.e., $\alpha=3.05$), and $s=1.0$ (i.e., $r=1.2096$). The diffusion coefficient $G(y)$ is continuous in $y=\pm Lr$ although its first derivative is discontinuous. The drift coefficient $H(y)$ suffers a discontinuity in $y=\pm Lr$. We recall that a finite discontinuity in the drift coefficient is not usually pathological for the solutions of the Fokker-Planck equation (see for example the V-shaped potential of Ref. [3]). As long as the probability current is concerned, it is straightforward to prove that the density current $J(y,t)$ in the new variables is simply given by $J(y,t)=j[f_g^{-1}(y),t]$, where $j(x,t)$ is the density current of the process of Eq. (5). The function f_g^{-1} is well defined because f_g is continuous and monotonic.

The autocorrelation function of the process defined by the coordinate transformation of Eq. (6) is given by $\rho_g(\tau)=(\langle y(t+\tau)y(t)\rangle-\langle y(t)\rangle^2)/(\langle y^2(t)\rangle-\langle y(t)\rangle^2)$, where

$$\langle y(t)y(t+\tau)\rangle = \int_0^\infty d\lambda \mathcal{C}_\lambda^2 e^{-\lambda\tau},$$

$$\mathcal{C}_\lambda = \int_{-\infty}^{+\infty} dx f_g(x)\psi_0(x)\psi_\lambda(x), \tag{7}$$

where $\psi_0(x)$ and $\psi_\lambda(x)$ are the eigenfunctions of the process of Eq. (5). Equation (7) can be used to numerically obtain the autocorrelation of the process defined by the coordinate transformation of Eq. (6).

In the top panel of Fig. 2 we report the results of the numerical integration of Eq. (7) for the case when $L=1.0$ and $s=1.0$, and the V_0 values are chosen in such a way that the parameter α assumes the values shown in the legend. The asymptotic behavior of these autocorrelation functions seems compatible with a power law $\tau^{-\beta_g}$. In the bottom panel of

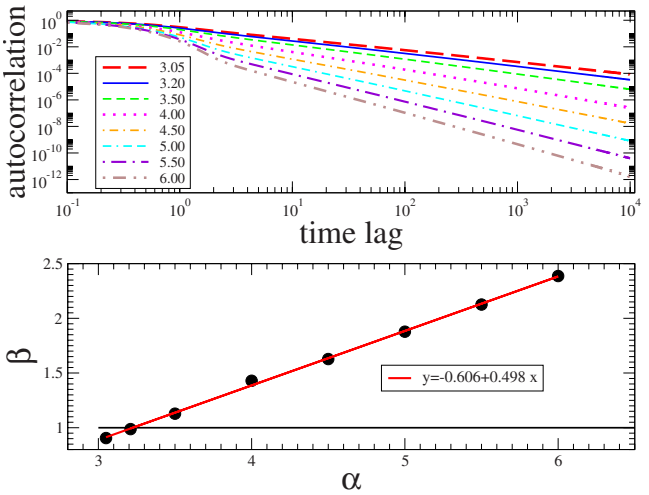

FIG. 2. (Color online) In the top panel we report the results of the numerical integration of Eq. (7) for the case when $L=1.0$ and $s=1.0$, and the V_0 values are chosen in such a way that the parameter α assumes the values shown in the legend. In the bottom panel we report the values of the exponents β_g obtained by performing a nonlinear fit of the autocorrelation function shown in the top panel.

Fig. 2 we report the values of the exponents β_g obtained by performing a nonlinear fit of the autocorrelation function shown in the top panel. Such values show a dependence from the α parameter which seems compatible with a linear law $\beta_g=\alpha/2-\eta_g$, with $\eta_g\approx 0.61$. For values $\alpha<2\eta_g+1$ we get $\beta_g<1$, i.e., the stochastic process thus generated is long-range correlated. It is worth noticing that the autocorrelation function $\langle y(t)y(t+\tau)\rangle$ does not show any dependence from the s parameter.

In the top panel of Fig. 3 we show the results of numerical simulations of the autocorrelation function performed for the case when $L=1.0$, $V_0=0.987$ (i.e., $\alpha=3.05$), and $s=1.0$ (i.e., $r=1.2096$). The solid (red) line shows the theoretical prediction obtained from Eq. (7), while the open circles show the result of the numerical simulations. By performing a nonlinear fit (dashed blue line), the autocorrelation function shows an asymptotic decay compatible with a power law $\tau^{-\beta_g}$, with $\beta_g=0.86$. In the inset of the top panel we show the numerical simulation (circles) relative to the mean-square displacement $\langle|\Delta s(t)|^2\rangle$, where $s(t)$ is the stochastic process obtained by integrating over time the process defined by the coordinate transformation of Eq. (6). A nonlinear fit (solid blue line) shows that $\langle|\Delta s(t)|^2\rangle\propto t^\delta$ with $\delta=1.21$, thus confirming that our process behaves like a superdiffusive long-range correlated stochastic process in the range where the numerical simulations were performed. The bottom panel of Fig. 3 shows the stationary pdf of the process. Again the solid (red) line shows the theoretical prediction of Eq. (6), while the open circles show the result of the numerical simulations. In the inset we show the same pdf in a shorter range of values in order to emphasize that inside the region $|y|\leq Lr$ the pdf has a behavior different from Gaussian.

Those shown in Fig. 3 are time-average numerical simulations performed according to the relation

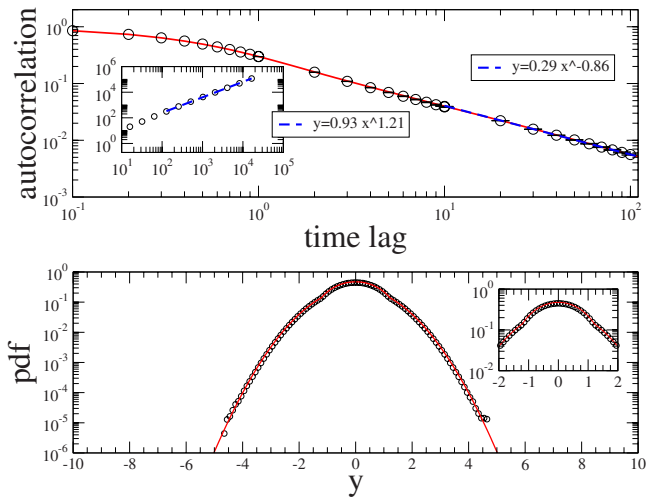

FIG. 3. (Color online) The figure shows time-average numerical simulations performed according to Eq. (9) performed for the case when $L=1.0$, $V_0=0.987$ (i.e., $\alpha=3.05$), and $s=1.0$ (i.e., $r=1.2096$). The simulation parameters are $M=10$ in the region $\tau\in[1,10]$ and $M=20$ in the region $\tau\geq 10$, $T=1.01\times 10^{11}$. The time step was $\Delta t=0.005$. In the top panel we show the results for the autocorrelation function. The solid (red) line shows the theoretical prediction obtained from Eq. (7), while the open circles show the result of the numerical simulations. By performing a nonlinear fit (dashed blue line), the autocorrelation function shows an asymptotic decay compatible with a power law $\tau^{-\beta_g}$, with $\beta_g=0.86$. In the inset of the top panel we show the numerical simulation (circles) relative to the mean-square displacement $\langle|\Delta s(t)|^2\rangle$. A nonlinear fit (solid blue line) shows that $\langle|\Delta s(t)|^2\rangle\propto t^{\delta}$ with $\delta=1.21$. The bottom panel shows the stationary pdf of the process. Again the solid (red) line shows the theoretical prediction of Eq. (6), while the open circles show the result of the numerical simulations.

$$\rho(\tau)=\frac{1}{T}\int_0^T dt x_*(t)x_*(t+\tau), \tag{8}$$

where T is the length of the simulated time series and $x_*(t)$ is one realization of the process. Indeed, in order to improve the statistical reliability of our numerical simulations, in the region $\tau\geq 1$ we have also averaged over a number M of different realizations of the process,

$$\rho_T(\tau)=\frac{1}{M}\sum_{j=1}^{M}\frac{1}{T}\int_0^T dt x_j(t)x_j(t+\tau). \tag{9}$$

The data shown in the figure are the mean and the standard deviations of the M autocorrelation values computed in each iteration for each time lag. The values of M are $M=10$ in the region $\tau\in[1,10]$ and $M=20$ in the region $\tau\geq 10$. The size of each time series was $T=1.01\times 10^{11}$ with a time step of $\Delta t=0.005$. The starting points of the simulated time series were all the same with $x_j(0)=0.1$, where $j=1,\ldots,M$. In order to simulate the process in the y coordinate space, we start by simulating the process of Eq. (5) and compute $y=f(x)$ for each simulated x value. However, we have explicitly checked that such procedure is equivalent to a direct simulation of the Langevin equation obtained starting from $H(y)$ and $G(y)$.

The existence of power-law correlated processes with Gaussian tails does not contradict the Doob Theorem [46]. In fact, such theorem deals with the case when the process admits stationary pdfs and two-point conditional transition probabilities which are both nonsingular and Gaussian on the whole real axis.

IV. EXPONENTIAL TAILS IN THE PDF

In this section we explicitly present a stationary Markovian process with a slowly decaying autocorrelation function and a stationary pdf with exponentially decaying tails. In fact, let us consider the coordinate transformation

$$f_e(x)=\begin{cases}\dfrac{1}{\gamma}\log[\gamma(x-L)+e^{\gamma L r}] & x>L\\ -\dfrac{1}{\gamma}\log[\gamma(-x-L)+e^{\gamma L r}] & x<-L\\ rx & |x|\leq L.\end{cases} \tag{10}$$

By using the Ito lemma, one can show that starting from the process of Eq. (5), in the coordinate space $y=f_e(x)$ one gets the multiplicative stochastic process described by

$$\dot{y}=H(y)+G(y)\Gamma(t),$$

$$H(y)=\begin{cases}-\gamma e^{-2\gamma y}\dfrac{(1+\alpha)e^{\gamma y}+\Lambda}{e^{\gamma y}+\Lambda} & |y|>Lr\\ -2r\sqrt{V_0}\tan(\sqrt{V_0}y/r) & |y|\leq Lr,\end{cases}$$

$$G(y)=\begin{cases}e^{-\gamma y} & |y|>Lr\\ r & |y|\leq Lr,\end{cases}$$

$$\Lambda=\gamma L-e^{\gamma L r}, \tag{11}$$

where r is a real positive constant which is fixed by imposing that the diffusion coefficient $G(y)$ is continuous in $y=\pm Lr$. It is straightforward to prove that such process admits the stationary pdf,

$$W_e(y)=\begin{cases}N_{\mathrm{I}}e^{-\gamma y}(\Lambda+e^{\gamma y})^{-\alpha} & |y|>Lr\\ N_{\mathrm{II}}\cos(\sqrt{V_0}y/r)^2 & |y|\leq Lr,\end{cases} \tag{12}$$

whose tails are asymptotically exponential. N_{I} and N_{II} are normalizations constants that can be analytically computed by imposing that $W_e(y)$ is continuous in $y=\pm Lr$ and it is normalized to unity.

The autocorrelation function of the process of Eq. (11) can be obtained starting from Eq. (7) with $f_g(x)$ now replaced by $f_e(x)$ of Eq. (10).

In the top panel of Fig. 4 we report the results of the numerical integration of Eq. (7) for the case when $L=1.0$ and $\gamma=1.0$, and the V_0 values are chosen in such a way that the parameter α assumes the values shown in the legend. The asymptotic behavior of these autocorrelation functions seems compatible with a power law $\tau^{-\beta_e}$. In the bottom panel of Fig. 4 we report the values of the exponents β_e obtained by performing a nonlinear fit of the autocorrelation function shown in the top panel. Such values show a dependence from

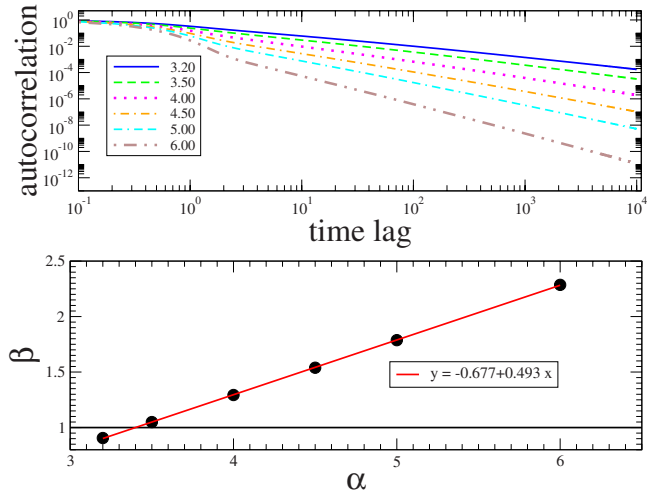

FIG. 4. (Color online) In the top panel we report the results of the numerical integration of Eq. (7) for the coordinate transformation of Eq. (10) when $L=1.0$ and $\gamma=1.0$, and the V_0 values are chosen in such a way that the parameter α assumes the values shown in the legend. In the bottom panel we report the values of the exponents β_e obtained by performing a nonlinear fit of the autocorrelation function shown in the top panel.

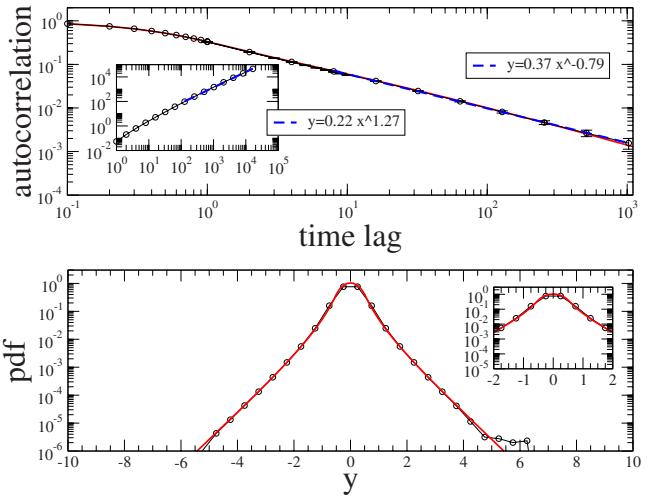

FIG. 5. (Color online) The figure shows time-average numerical simulations performed according to Eq. (9) performed for the case when $L=1.0$, $V_0=1.020$ (i.e., $\alpha=3.21$), and $\gamma=1.0$ (i.e., $r=0.567$). The simulation parameters are $M=10$ in the region $\tau\in[1,10]$ and $M=20$ in the region $\tau\geq 10$, $T=1.025\times 10^{11}$. The time step was $\Delta t=0.01$. In the top panel we show the results for the autocorrelation function. The solid (red) line shows the theoretical prediction obtained from Eq. (7), while the open circles show the result of the numerical simulations. By performing a nonlinear fit (dashed blue line), the autocorrelation function shows an asymptotic decay compatible with a power law $\tau^{-\beta_e}$, with $\beta_e=0.79$. In the inset of the top panel we show the numerical simulation (circles) relative to the mean-square displacement $\langle|\Delta s(t)|^2\rangle$. A nonlinear fit (solid blue line) shows that $\langle|\Delta s(t)|^2\rangle\propto t^{\delta}$ with $\delta=1.26$. The bottom panel shows the stationary pdf of the process. Again the solid (red) line shows the theoretical prediction of Eq. (12), while the open circles show the result of the numerical simulations.

the α parameter which seems compatible with a linear law $\beta_e=\alpha/2-\eta_e$, with $\eta_e\approx 0.68$. Differently form the Gaussian case, now the autocorrelation function $\langle y(t)y(t+\tau)\rangle$ seems to show some dependence from the γ parameter. As an example, we have computed the autocorrelation functions for the same values as above and with $\gamma=1.0$ replaced by $\gamma=10.0$. Again we find that η depends upon α according to a linear law $\beta_e=\alpha/2-\eta_e$, where now $\eta_e\approx 0.62$.

In the top panel of Fig. 5 we show the results for the case when $L=1.0$, $V_0=1.020$ (i.e., $\alpha=3.21$), and $\gamma=1.0$ (i.e., $r=0.567$). The solid (red) line shows the theoretical prediction obtained from Eq. (7), while the open circles show the result of the numerical simulations. By performing a nonlinear fit (dashed blue line), the autocorrelation function shows an asymptotic decay compatible with a power law $\tau^{-\beta_e}$, with $\beta_e=0.79$. In the inset of the top panel we show the numerical simulation (circles) relative to the mean-square displacement $\langle|\Delta s(t)|^2\rangle$, where $s(t)$ is the stochastic process obtained by integrating over time the process defined by the coordinate transformation of Eq. (10). A nonlinear fit (solid blue line) shows that $\langle|\Delta s(t)|^2\rangle\propto t^{\delta}$ with $\delta=1.26$, thus confirming that our process behaves like a superdiffusive long-range correlated stochastic process in the range where the numerical simulations were performed. The bottom panel of Fig. 5 shows the stationary pdf of the process. Again the solid (red) line shows the theoretical prediction of Eq. (12), while the open circles show the result of the numerical simulations. In the inset we show the same pdf in a shorter range of values in order to emphasize that inside the region $|y|\leq Lr$ the pdf has a behavior different from exponential.

Those shown in Fig. 5 are time-average numerical simulations performed according to Eq. (8). Differently from the previous case, when simulating the process we directly consider the Langevin equation of Eq. (11). Again, in order to improve the statistical reliability of our numerical simulations, in the region $\tau>1$ we have also averaged over a number M of different realizations of the process, according to Eq. (9). The data shown in the figure are the mean and the standard deviations of the M autocorrelation values computed in each iteration for each time lag. The values of M are $M=10$ in the region $\tau\in[1,10]$ and $M=20$ in the region $\tau\geq 10$. The size of each time series was $T=1.025\times 10^{11}$ with a time step of $\Delta t=0.01$. The starting points of the simulated time series were all the same with $x_j(0)=0.1$, where $j=1,\ldots,M$.

V. AUTOCORRELATION ASYMPTOTIC DECAY AND TAILS IN THE PDF

Let us consider a generic coordinate transformation $y=f(x)$, where $f(x)$ is a continuous monotonously increasing function. The autocorrelation function $\langle y(t)y(t+\tau)\rangle$ is given by Eq. (7) with $f_g(x)$ replaced by the $f(x)$. It is in general quite hard to analytically perform the various integration required in Eq. (7). However, one can obtain asymptotic results that are valid in the large time limit. As illustrated in Ref. [45], the large time behavior of $\langle y(t)y(t+\tau)\rangle$ is determined by the small energy behavior of $\mathcal{C}_\lambda=\int_{-\infty}^{+\infty}dx f(x)\psi_0(x)\psi_\lambda(x)$. The main contribution to $\mathcal{C}_\lambda$ comes from the integration in the domain $[L,\infty]$.

By performing the change of variable $x=1/v$ and $\sqrt{\lambda}=1/\xi$ one gets

$$\mathcal{C}_\lambda = A_0 A_\lambda \int_0^{1/L} dv v^{(\alpha-5)/2} f\left(\frac{1}{v}\right) J_\nu\left(\frac{1}{v\xi}\right), \tag{13}$$

where we used the explicit form of ψ_0 and ψ_λ given in Sec. II. In principle, in Eq. (13) one should consider a contribution depending from $Y_\nu(\cdot)$. However, one can explicitly show that such contribution is of the same order as the one we are already considering.

Equation (13) makes it clear that the small energy behavior of $\mathcal{C}_\lambda$ strictly depends on the specific shape of the coordinate transformation $f(x)$ at large x values. As an illustrative example we will consider the coordinate transformation of Eq. (10).

We preliminary observe that

$$\int dv g(\xi v) v^{\mu-1} \log v = \frac{G'(\mu) - G(\mu)\log \xi}{\xi^\mu}, \tag{14}$$

where $G(\cdot)$ is the Mellin transformation of the function $g(\cdot)$ and $G'(\cdot)$ is its first derivative. In the case of $g(\xi v)=J_\nu[1/(v\xi)]$ we get

$$G(z) = \frac{1}{2^{1+z}} \frac{\Gamma[(\nu-z)/2]}{\Gamma[1+(\nu+z)2]}. \tag{15}$$

The above result, together with those reported in chapter 9 of Ref. [45], allows us to conclude that the small energy behavior of $\mathcal{C}_\lambda$ is given by

$$\begin{aligned}\mathcal{C}_\lambda \approx{}& \frac{A_0}{\gamma}\left[G\left(\frac{\alpha-3}{2}\right)\log\gamma - G'\left(\frac{\alpha-3}{2}\right)\right]\lambda^{(\alpha-3)/4} \\ &+ \frac{A_0}{2\gamma} G\left(\frac{\alpha-3}{2}\right)\lambda^{(\alpha-3)/4}\log\lambda \\ &+ A_0 \sum_{s=1}^{\infty} a_s G\left(s+\frac{\alpha-3}{2}\right)\lambda^{(\alpha-3)/4+s/2},\end{aligned} \tag{16}$$

where $a_s=(-\Lambda)^s/(s\gamma^{s+1})$. By using the Watson lemma and the results in chapter 9 of Ref. [45] one finally gets

$$\begin{aligned}\langle y(t)y(t+\tau)\rangle \approx{}& C_0 \frac{1}{\tau^{(\alpha-1)/2}} + C_1 \frac{1}{\tau^{(\alpha-1)/2}}\log\tau \\ &+ C_2 \frac{1}{\tau^{(\alpha-1)/2}}(\log\tau)^2 + \cdots,\end{aligned} \tag{17}$$

where the other terms in the series expansion are of the order of $\tau^{(\alpha-1)/2+s/2}$ or $\tau^{(\alpha-1)/2+s/2}\log\tau$ with $s=1,2,3,\ldots$. The coefficients $C_0, C_1, C_2, \ldots$ in the above expansion can be easily computed in terms of the coefficients of the asymptotic expansion of Eq. (16). When $\alpha<3$ the process is long-range correlated.

The above result must be compared with the numerical one shown in Fig. 4. In that case we found that the asymptotic behavior of the autocorrelation function is compatible with a power-law behavior $\tau^{-\beta_e}$ with $\beta_e=\alpha/2-\eta_e$ and $\eta_e\approx 0.68$. The result of Eq. (17) confirms the $\alpha/2$ dependence in the power-law exponent. However, the value of η_e does not have a correspondence in the analytical result of Eq. (17). This is no surprise since Eq. (17) predicts a logarithmic correction to the power law that is usually quite hard to detect numerically. Moreover, the coefficients $C_0, C_1, C_2, \ldots$ in the asymptotic expansion of Eq. (17) are of comparable magnitude. Therefore, in the range where the numerical integrations were performed one expects to see a combination of power laws (with logarithmic corrections), rather than a single one. These results are in qualitative agreement with those of Ref. [47].

Equation (13) also makes it clear what is the relationship between the large time behavior of the autocorrelation function and the tails of the stationary pdf:

$$W(y) = \frac{1}{f'(x)} A_0^2 \frac{1}{x^\alpha}\bigg|_{x=f^{-1}(y)}. \tag{18}$$

In fact, the large time behavior of $\langle y(t)y(t+\tau)$ is determined by the behavior of $f(1/v)$ for small values of v, i.e., the behavior of $f(x)$ for large values of x. Since $y=f(x)$ is continuous and monotonously increasing we have that the large values of x are mapped into large values of y. Therefore the asymptotic behavior of $f(x)$ for large values of x determines the behavior of the stationary pdf in the new variables $W(y)$ for large values of y.

Suppose that $f(x)$ admits a power-law series expansion for small values of $v=1/x$: $f(x)\approx\Sigma_s a_s v^s$. Then, by using the results in Ref. [45] one can prove that the autocorrelation function behaves like $\langle y(t)y(t+\tau) \approx \Sigma_s R_s 1/\tau^{s+(\alpha-1)/2}$. At the same time, one can also prove that the stationary pdf admits power-law tails. In fact, the existence of the above series expansions guarantees that the derivatives $\partial^n f^{-1}(y)/\partial y^n$ are well defined for $1/y\to 0$. For example, in the simple case when $y=x^a$, then $W(y)\approx y^{(\alpha+a-1)/a}$ and $\langle y(t)y(t+\tau) \approx \tau^{a+(\alpha-5)/2}$. In this case we have a stationary Markovian power-law correlated process that is in the basin of attraction of the Frechet distribution [35]. This is an example, in the context of stationary Markovian processes, of the model proposed in Ref. [37], where long-range dependencies are shown to explain the clustering of extreme events.

Whenever $f(x)$ admits a series expansion for small values of $v=1/x$ which is not purely in terms of power laws then one can have stationary Markovian processes which are possibly long-range correlated and whose stationary pdf shows tails which are not algebraic for large values of y, as in the explicit examples of Secs. III and IV. In this case the processes are in the basin of attraction of the Gumbel distribution [35]. These examples show that long-range dependencies are possible without necessarily having clustering of extreme events.

VI. CONCLUSIONS

We have shown stationary Markovian processes that are long-range correlated and have a stationary pdf with tails that can be Gaussian and asymptotically exponential. The processes are obtained by simply performing a coordinate transformation of the additive process described in Eq. (5). Start-

ing from such specific process, we have given (i) analytical evidence that the considered processes have the mentioned stationary pdfs and (ii) numerical evidence that the decay of the autocorrelation function is compatible with a power law $\langle y(t)y(t+\tau)\rangle \propto \tau^{-\beta}$, where $\beta=\alpha/2-\eta$ and η is a parameter that depends from the specific tails of the stationary pdf. The above linear law holds true also in the case of the additive process of Eq. (5), with $\eta=3/2$. This numerical result is partially confirmed by the analytical calculations of Sec. V, where in the case of the process of Sec. IV it is explicitly shown that the autocorrelation function decays with a power law $\tau^{-(\alpha/2-0.5)}$ with logarithmic corrections.

It is worth remarking that in principle more general processes can be obtained (i) by choosing different coordinate transformations or (ii) by appropriately engineering the shape of the quantum potential $V_S(x)$ of Eq. (5) in the region $[-L,L]$. This would result in a different shape of the stationary pdf in that region. When doing that, the asymptotic behavior of the autocorrelation function is not modified. In this paper we preferred to consider a linear transformation and $V_S(x)=-V_0$ in the region $[-L,L]$ only because this allows us to analytically obtain the eigenfunctions on the whole real axis and to obtain a numerical theoretical prediction for the autocorrelation function of the stochastic processes considered.

Starting from the process of Eq. (5), stationary pdfs with tails different from exponential or Gaussian ones can be obtained by introducing appropriate coordinate transformations. In all cases the autocorrelation functions can be obtained by using the same approach illustrated in this paper.

It is worth remarking that the existence of power-law correlated processes with Gaussian tails does not contradict the Doob theorem [46] because the Doob theorem deals with the case when the process admits a stationary pdf and a two–point conditional transition probability which are both Gaussian on the whole real axis and non singular. In our case we only have Gaussian tails in the stationary pdf.

Our results help in clarifying that even in the context of stationary Markovian processes long-range dependencies are not necessarily associated to the occurrence of extreme events. In fact, the processes introduced in Secs. III and IV are in the basin of attraction of the Gumbel distribution [35], although the one of Eq. (5) is in the basin of attraction of the Frechet distribution. In Sec. V we have analytically investigated on the general relationship between the large time behavior of the autocorrelation function and the tails of the stationary pdf. Specifically, by performing a coordinate transformation $y=f(x)$, where $f(x)$ admits a power-law series expansion at infinity one gets processes with power-law tails in the stationary pdf and power-law correlated. When $f(x)$ does not admit a series expansion purely in terms of power laws then one can have stationary Markovian processes which are possibly long-range correlated and whose stationary pdf show tails which are not power law for large values of y. Our results seem thus to neglect the possibility of performing a coordinate transformation that generates power-law correlated processes belonging to the basin of attraction of the Gumbel distribution, although long-range correlated processes are possible. In other words, extreme events seem to be associated to long-range correlated processes with power-law decaying autocorrelation function. However, the occurrence of extreme events is not necessary in order to have more general long-range correlated processes in which the autocorrelation shows a slow decay characterized by a power law times a correction function such as the logarithm found in Sec. V.

Our results can be relevant in the modeling of complex systems with long memory. In fact, processes with long-range interactions are often modeled by means of the Fractional Brownian motion (FBm), multifractal processes, memory kernels, and other. Here we provide simple stationary processes associated to Langevin equations with white noise, thus confirming that memory effects can still be modeled in the context of continuous time stationary Markovian processes, i.e., even assuming the validity of the Chapman-Kolmogorov equation.

[1] A. Einstein, Ann. Phys. **17**, 549 (1905); M. V. Smoluchowski, Phys. Z. **17**, 557 (1916).

[2] N. G. Van Kampen, *Stochastic Processes in Physics and Chemistry* (Elsevier, Amsterdam, 1981).

[3] H. Risken, *The Fokker-Planck Equation* (Springer, Berlin, 1989).

[4] C. W. Gardiner, *Handbook of Stochastic Methods* (Springer-Verlag, Berlin, 1985).

[5] Z. Schuss, *Theory and Application of Stochastic Differential Equations* (Wiley, Toronto, 1980).

[6] B. Oksendal, *Stochastic Differential Equations: An Introduction with Applications* (Springer, Berlin, 2003).

[7] M. S. Waterman, *Mathematical Methods for DNA sequences* (CRC Press, Boca Raton, FL, 1989).

[8] R. Durbin, S. Eddy, A. Krogh, and G. Mitchison, *Biological Sequence Analysis* (Cambridge University Press, Cambridge, 2001).

[9] J.-P. Bouchaud and M. Potters, *Theory of Financial Risk and Derivative Pricing: From Statistical Physics to Risk Management* (Cambridge University Press, Cambridge, 2003).

[10] R. N. Mantegna and E. Stanley, *Introduction to Econophysics* (Cambridge University Press, Cambridge, 1999).

[11] H. von Storch and F. W. Zwiers, *Statistical Analysis in Climate Research* (Cambridge University Press, Cambridge, 2002).

[12] D. Helbing, *Quantitative Sociodynamics: Stochastic Methods and Models of Social Interaction Processes* (Kluver Academic Publishers, Dordrecht, 1995).

[13] J. Beran, *Statistics for Long-Memory Processes* (Chapman and Hall, London, 1994).

[14] M. Cassandro and G. Jona-Lasinio, Adv. Phys. **27**, 913 (1978).

[15] J.-P. Bouchaud and A. Georges, Phys. Rep. **195**, 127 (1990).

[16] G. Samorodnitsky and M. S. Taqqu, *Stable Non-Gaussian Random Processes: Stochastic Models with Infinite Variance* (Chapman and Hall, New York, 1994).

[17] R. Metzler and J. Klafter, Phys. Rep. **339**, 1 (2000).
[18] R. Metzler and J. Klafter, J. Phys. A **37**, R161 (2004).
[19] L. F. Richardson, Proc. R. Soc. London, Ser. A **110**, 709 (1926).
[20] T. Geisel, J. Nierwetberg, and A. Zacherl, Phys. Rev. Lett. **54**, 616 (1985).
[21] A. Ott, J.-P. Bouchaud, D. Langevin, and W. Urbach, Phys. Rev. Lett. **65**, 2201 (1990).
[22] T. H. Solomon, E. R. Weeks, and H. L. Swinney, Phys. Rev. Lett. **71**, 3975 (1993).
[23] C. Peng, S. V. Buldyrev, A. L. Goldberger, S. Havlin, F. Sciortino, M. Simons, and H. E. Stanley, Nature (London) **356**, 168 (1992).
[24] Y. Liu, P. Gopikrishnan, P. Cizeau, M. Meyer, C.-K. Peng, and H. E. Stanley, Phys. Rev. E **60**, 1390 (1999).
[25] E. W. Montroll and G. H. Weiss, J. Math. Phys. **6**, 167 (1965).
[26] R. Kubo, Rep. Prog. Phys. **29**, 255 (1966).
[27] B. B. Mandelbrot and J. W. van Ness, SIAM Rev. **10**, 422 (1968).
[28] M. F. Shlesinger, G. M. Zaslavsky, and J. Klafter, Nature (London) **363**, 31 (1993).
[29] M. H. Vainstein, I. V. L. Costa, R. Morgado, and F. A. Oliveira, Europhys. Lett. **73**, 726 (2006).
[30] H. G. E. Hentschel and I. Procaccia, Phys. Rev. A **29**, 1461 (1984).
[31] G. E. Uhlenbeck and L. S. Ornstein, Phys. Rev. **36**, 823 (1930).
[32] S. Marksteiner, K. Ellinger, and P. Zoller, Phys. Rev. A **53**, 3409 (1996).
[33] E. J. Gumbel, Ann. Inst. Henri Poincare **5**, 115 (1935).
[34] B. V. Gnedenko, Ann. Math. **44**, 423 (1943).
[35] P. Embrechts, C. Kluppelberg, and T. Mikosch, *Modelling Extremal Events* (Springer-Verlag, Berlin, 1997).
[36] S. Albeverio, V. Jentsch, and H. Kantz, *Extreme Events in Nature and Society* (Springer, New York, 2006).
[37] A. Bunde, J. F. Eichner, J. W. Kantelhardt, and S. Havlin, Phys. Rev. Lett. **94**, 048701 (2005).
[38] E. Lutz, Phys. Rev. Lett. **93**, 190602 (2004).
[39] F. Lillo and R. N. Mantegna, Phys. Rev. Lett. **84**, 1061 (2000).
[40] A. Schenzle and H. Brand, Phys. Rev. A **20**, 1628 (1979).
[41] M. Suzuki, K. Kaneko, and F. Sasagawa, Prog. Theor. Phys. **65**, 828 (1981).
[42] R. Graham and A. Schenzle, Phys. Rev. A **25**, 1731 (1982).
[43] W. Horsthemke and R. Lefever, *Noise Induced Transitions* (Springer-Verlag, Berlin, 1984).
[44] J. Farago, Europhys. Lett. **52**, 379 (2000).
[45] F. W. J. Olver, *Asymptotics and Special Functions* (Academic Press, New York, 1974).
[46] J. L. Doob, Ann. Math. **43**, 351 (1942).
[47] P. H. Chavanis and M. Lemou, Eur. Phys. J. B **59**, 217 (2007).